Oriented Object Detection with Transformer

Teli Ma[1,†], Mingyuan Mao[2,†], Honghui Zheng[3], Peng Gao[3], Xiaodi Wang[3], Shumin Han[3,*],
Errui Ding[3], Baochang Zhang[2], David Doermann[1,*]
[1]University at Buffalo, Buffalo, USA
[2]Beihang University, Beijing, China
[3]Department of Computer Vision Technology (VIS), Baidu Inc
[*]Corresponding author, email: hanshumin@baidu.com, doermann@buffalo.edu
[†]Equal contributions

Abstract

Object detection with Transformers (DETR) has achieved a competitive performance over traditional detectors, such as Faster R-CNN. However, the potential of DETR remains largely unexplored for the more challenging task of arbitrary-oriented object detection problem. We provide the first attempt and implement Oriented Object DEtection with TRansformer ($\mathbf{O^2DETR}$) based on an end-to-end network. The contributions of O^2DETR include: 1) we provide a new insight into oriented object detection, by applying Transformer to directly and efficiently localize objects without a tedious process of rotated anchors as in conventional detectors; 2) we design a simple but highly efficient encoder for Transformer by replacing the attention mechanism with depthwise separable convolution, which can significantly reduce the memory and computational cost of using multi-scale features in the original Transformer; 3) our O^2DETR can be another new benchmark in the field of oriented object detection, which achieves up to 3.85 mAP improvement over Faster R-CNN and RetinaNet. We simply fine-tune the head mounted on O^2DETR in a cascaded architecture and achieve a competitive performance over SOTA in the DOTA dataset.

1 Introduction

Arbitrary-oriented targets are widely distributed in application scenarios like scene text detection and remote sensing object detection (Xia et al., 2018). Detecting oriented targets with anchors without rotation is difficult as targets are always tiny, oblique and densely packed. Based on that, many rotated detectors like R^3Det (Yang et al., 2019a), S^2ANet (Han et al., 2020), ReDet (Han et al., 2021) are proposed to detect objects based on traditional detectors like Faster R-CNN (Ren et al., 2016), RetinaNet (Lin et al., 2017b) by adding rotation of pre-set anchors while learning. However, the rotated-anchor regression and post-process like non-maximum suppression are based on a tedious and redundant process, which is an indirect and sub-optimal solution to the oriented object detection problem.

In this paper, based on Transformer (Vaswani et al., 2017) and DETR (Carion et al., 2020), we introduce an Oriented Object DEtection with TRansformer ($\mathbf{O^2DETR}$) method, which is the first attempt to apply Transformer to the oriented object detection task. We provide a direct method for oriented object detection by matching angled boxes with oriented objects end-to-end as shown in Fig. 1. Specifically, we pre-set and improve the fixed-length object queries with angle dimension to interact with the encoded features, and extract angle-dimensional information via cross-attention mechanism. The set of angle-aware object queries match ground truths with bipartite matching during training.
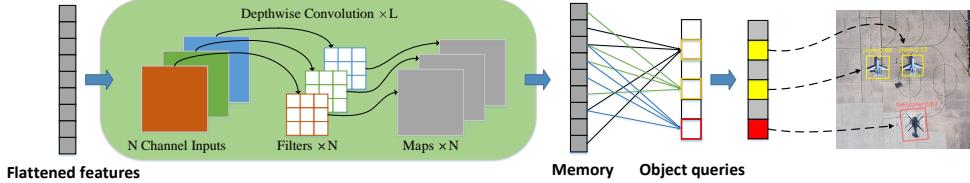
Figure 1: The end-to-end scheme of O^2DETR

Considering significant scale variances for different categories of oriented objects (large ones like ground-track-field and tiny ones like small-vehicle), multi-scale feature maps are necessary for object detection. However, global reasoning scheme of attention mechanism of the original Transformer encoder is highly and computationally complex for multi-scale features. Furthermore, we argue that global reasoning is actually not necessary, especially when oriented objects of the same category are always densely packed and the object query only interacts with visual features around the object rather than those of whole global image. Based on these observation, we are inspired to introduce local aggregation with depthwise separable convolutions which can perform much better than the original self-attention mechanism of Tranformer. Replacing with convolutions shortens the Transformer training epochs and achieves a fast convergence compared with the conventional attention mechanism, because the information exchange only happens among adjacent pixels when extracting features.

Experiments on DOTA (Xia et al., 2018) dataset demonstrate our O^2DETR outperforms both one-stage and two-stage rotated detectors without any refinement by 3.85% mAP. Based on that, we fine-tune the head mounted on O^2DETR with a cascaded refinement module to boost performance of our detector further. With parameters of Transformer fixed, we use predictions of O^2DETR as the region proposal and select features from feature maps generated by backbone to fine-tune a cascaded prediction head as shown in Fig. 2. We only fine-tune the head and achieve 79.66% mAP on DOTA test dataset with backbone ResnNet-50, leading to a competitive performance compared with the state-of-the-art.

2 Related Works

Oriented Object Detection. Oriented object detection refers to building detectors using rotated bounding box representation. Arbitrary-oriented targets are widely distributed in remote sensing and text images. These targets are often crowded, distribute with large scale variations and appear at arbitrary orientations (Xia et al., 2018). Thus, existing methods built on detectors using horizontal bounding boxes suffer from containing several objects of interest in one anchor/RoI. Some methods are adopted to alleviate the problem. R-RPN (Ma et al., 2018) uses rotated region proposal networks to detect oriented targets by rotated proposals. In R^2CNN (Jiang et al., 2017), a horizontal region of interest (RoI) is leveraged to predict both horizontal and rotated boxes. RoI Transformer (Ding et al., 2019) transforms the horizontal RoI in R^2CNN into a rotated one (RRoI). SCRDet (Yang et al., 2019b) and RSDet (Zhou et al., 2020) focus on boundary problem caused by periodicity of angle and propose novel losses to fix it. In CSL (Yang and Yan, 2020), angle regression is converted into classifying accurate angle value in one period. R^3Det (Yang et al., 2019a) samples features from center and corners of the corresponding anchor box and sum them up to re-encode the position information in order to solve misalignment of classification and localization. S^2A-Net (Han et al., 2020) uses aligned convolution network to refine the rotated boxes and align features. Recently proposed ReDet (Han et al., 2021) incorporates rotation-equivariant network into detector to extract rotation-equivariant features. To the best of our knowledge, all previous rotated detectors make predictions in a indirect way of rotating anchors or proposals rather than predicting with angle knowledge directly as our O^2DETR.

Transformers. Transformers (Vaswani et al., 2017) include both self-attention and cross-attention mechanism and achieve success in not only machine translation Gao et al. (2020); Ott et al. (2018), but also model pretraining (Brown et al., 2020; Devlin et al., 2018; Radford et al., 2018, 2019), visual recognition (Dosovitskiy et al., 2020; Mao et al., 2021; Ramachandran et al., 2019) and multi-modality fusion (Gao et al., 2019a,b; Geng et al., 2020; Lu et al., 2019; Yu et al., 2019). Transformers perform information exchange between all sets of inputs using key-query value attention. The
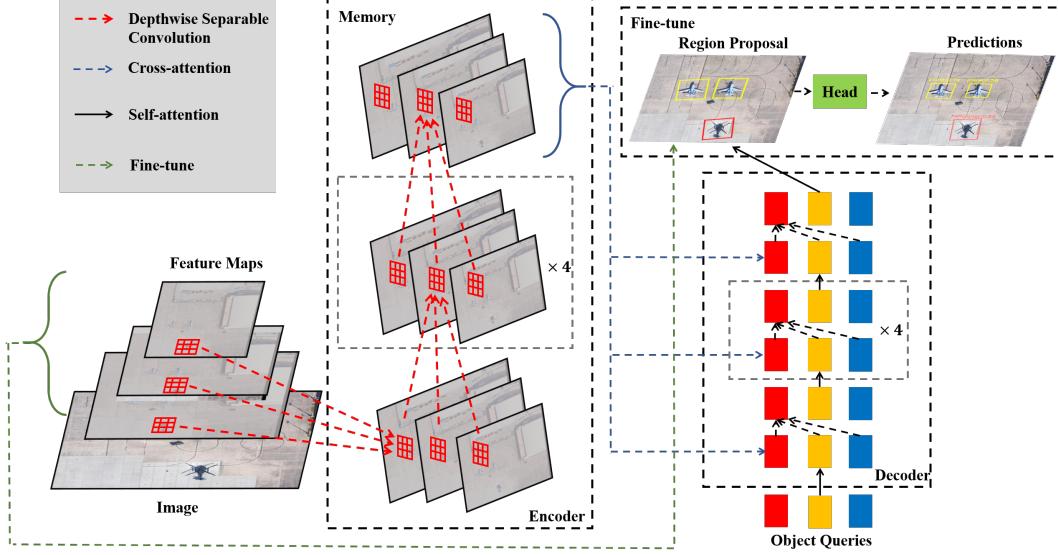
Figure 2: Illustration of the proposed O^2DETR and fine-tune method.

complexity of information exchange hinders model scalability in many cases for limiting input sequences. Many methods have been proposed to solve the problem. Reformer (Kitaev et al., 2020) proposes a reversible FFN and clustering self-attention. Linformer (Wang et al., 2020) and FastTransformer (Katharopoulos et al., 2020) propose to remove the softmax in the transformer and perform matrix multiplication between query and value first to obtain a linear-complexity transformer. Adaptive Clustering Transformer(ACT) (Zheng et al., 2020) perform an approximated self-attention by clustering key and query feature. LongFormer (Beltagy et al., 2020) perform self-attention within a local window instead of the whole input sequence. In Deformable DETR (Zhu et al., 2020), attention mechanism works on limited sample points rather than all image pixels, thus reduces training epochs largely compared with DETR (Carion et al., 2020). In SMCA-DETR (Gao et al., 2021), a spatially-modulated Gaussian mechanism has been introduced to coupled attention map with the position of predicted bounding-box and achieve fast convergence speed compared with DETR. In our model, we utilize depthwise separable convolutions to replace self-attention mechanism used in encoder to speed up training and save memory.

Depthwise Separable Convolution. Depthwise separable convolutions were first studied by (Sifre and Mallat, 2013) from Google Brain. In 2016, it was demonstrated a great success on large-scale image classification in Xception (Chollet, 2017). Later, the depthwise separable convolutions proved to reduce the number of parameters of models (the MobileNets family of architectures (Howard et al., 2017)) considerably. A depthwise separable convolution consists in a depthwise convolution, i.e. a spatial convolution performed independently over each channel of an input, followed by a pointwise convolution, i.e. a 1×1 convolution projecting the channels output of the depthwise convolution onto a new channel space. Previous work on depth-wise research focus on the light-weight characterstic. Our research show that the strong contextual aggregation ability of depthwise convolution than strong models like attention and deformable attention.

3 Method

O^2DETR is the first Transformer baseline in the oriented object detection domain to our best knowledge. Different from detecting oriented objects by rotating pre-set anchors to match objects, O^2DETR predicts rotated boxes directly from a set of object queries. Our work can be concluded as two points:

- Utilize separable depthwise convolutions to replace attention mechanism for an efficient Transformer encoder.

- Take advantage of high recall rate achieved by our O^2DETR to fine-tune the baseline for a better performance.

In the rest of the section, we discuss the setup process in details to show the process of constructing the model step by step.

3.1 Depthwise Separable Convolution and Attention

The original attention mechanism is computationally complex when processing multi-scale feature maps due to the global reasoning scheme, which is designed to capture relationships among all feature points in a global image. Differently, the depthwise convolution is proposed to for light-weight characteristic research, which shows the strong contextual aggregation and visual expression ability. The depthwise separable convolution operation consists of a depthwise convolution, which is a spatial convolution performed independently over every channel of the input, followed by a pointwise convolution with 1×1 filters projecting the channels computed by former depthwise convolution into new channel space. The formulation of a convolution operation is given as:

$$Conv(W, y)_{(i,j)} = \sum_{k,l,c}^{K,L,C} W_{(k,l,c)} \cdot y_{(i+k,j+l,c)}, \tag{1}$$

where K, L denote kernel size of convolution filter and the $y_{(i+k,j+l,c)} \in \mathbb{R}^1$ denotes a spatial feature point on cth ($c \in C$, input feature dimensions) channel. Then the depthwise separable convolution ($DSConv$ for abbreviation) can be formulated as:

$$DepthwiseConv(W, y)_{(i,j)} = \sum_{k,l}^{K,L} W_{(k,l)} \odot y_{(i+k,j+l)},$$

$$PointwiseConv(W, y)_{(i,j)} = \sum_{c}^{C} W_c \cdot y_{(i,j,c)}, \tag{2}$$

$$DSConv(W_p, W_d, y)_{(i,j)} = PointwiseConv_{(i,j)}(W_p, DepthwiseConv_{(i,j)}(W_d, y)),$$

where $\odot$ means the element-wise product and $y_{(i+k,j+l)} \in \mathbb{R}^C$ denotes a feature point in all channels. $DepthwiseConv(W, y)_{(i,j)} \in \mathbb{R}^{(H,W) \times C}$ denotes feature space generated by depthwise convolution and $PointwiseConv(W, y)_{(i,j)}$ denotes spatial feature space after utilizing pointwise convolution on results of depthwise convolution.

From Eq. 2 we can see the core idea of depthwise separable convolution which divides the feature learning into two separate steps, one is the spatial feature learning and the other is channel interaction. Then essence of such mechanism is to flatten and weight features of each channel. By comparison, the attention mechanism of Transformer consists of information exchange between the set of query and key elements. Given a set of query elements and a set of key elements, the attention mechanism adaptively aggregate the key contents according to the attention weights based on the measurement of compatibility of query-key pairs. The visual features are captured according to the attention weights, resulting in visual feature points interacting with others in the global image space. Let $\Omega_q \in \mathbb{R}^{H \times W}$ and $\Omega_k \in \mathbb{R}^{H \times W}$ represent the set of query and key elements, when $q \in \Omega_q$, $k \in \Omega_k$ index a query element wih representation feature $y_q \in \mathbb{R}^C$ and a key element with representation feature $y_k \in \mathbb{R}^C$. The attention feature is calculated as follow:

$$Attn(y_q, \mathbf{y}_{\Omega_k}) = \sum_{k \in \Omega_k} A_{(q,k)} \cdot W \odot y_k, \tag{3}$$

where $W \in \mathbb{R}^C$ is of learnable weights and attention weights A_{qk} are normalized as $\sum_{k \in \Omega_k} A_{(q,k)} = 1$. In the visual Transformer filed, the representation features y_q and y_k are usually of the concatenation/summation of element contents and positional embedding for $2D$ positional meaning. y_q and y_k are visual feature points in all channels with position embedding and apply dot multiplication, which is more similar to depthwise convolution rather than conventional convolution.

The depthwsie separable convolution is more efficient than attention mainly in the sampling space of visual feature points. To every query feature y_q, $Attn(y_q, x)$ do visual information interaction

with all key features through attention weights $A_{(q,k)}$, while the $W_{k,l}$ of depthwise convolution works on every feature map point $y_{(i,j)}$ to interact with local feature points around. We hypothesize the local aggregation of depthwise convolution performs better on tiny and dense objects, avoiding long training schedules before convergence of global feature interaction. Meanwhile, the depthwise separable convolutions reduce the complexity of model compared with attention mechanism. Suppose the channels, width, height of a feature map as C, W, H, the complexity of attention mechanism is $\mathcal{O}(HWC^2)$, while the complexity of depthwise separable convolution turns out to be $\mathcal{O}(kC + C^2)$ (k is the kernel size of filter and $k << HW$). It is safe to say replacing attention mechanism with depthwise separable convolution could save parameters and fasten training.

3.2 O^{2}DETR

Multi-scale Feature Presentation. Most oriented object detectors utilize multi-scale feature maps due to large variance of objects scales. Our proposed O^{2}DETR adopts multi-scale feature maps generated by backbone to enrich visual feature presentation. Given an input image, the encoder extracts the multi-scale visual features from the output feature maps $\{x^l\}_{l=1}^{L-1}$ of stages C_3 through C_5 in ResNet (He et al., 2016), where C_l is of resolution 2^l lower than the input image. The lowest resolution feature map x^L is obtained via a 3×3 and stride 2 convolution on the final C_5 stage, and denoted as C_6. All the feature maps of different scales are of 256 channels. Transformer encoder encodes all locations of different scales in multi-scale feature maps by propagating and aggregating information between pixels of different scales. The large number of pixels demonstrates the feasibility of replacing attention mechanism with convolution in encoding tokens. Specifically, we sum features from the adjacent levels into each level to fuse the different scale features for information fluid to acquire more semantic information, which is formulated as

$$DSConv(W_p, W_d, x)^l = DSConv(W_p, W_d, x)^l + \textbf{Dropout}(DSConv(W_p, W_d, x)^{l-1} \\ + DSConv(W_p, W_d, x)^{l+1}), \quad l \in [1, L-1]. \tag{4}$$

Given the encoded multi-scale features E_l ($l \in L$), multi-scale cross-attention is conducted between object query and feature maps. For each object query, a $2D$ normalized coordinate of the reference point p is predicted from original object query embedding calculated by linear project layers. The object queries extract multi-scale features from the encoder memory as

$$MSAttn(z_q, p, \{E_l\}_{l=1}^L) = \sum_{l=1}^{L} \sum_{k \in \Omega_k} A_{(q,k,l)} \cdot W \cdot x_k^l, \tag{5}$$

where visual features are taken from multiple levels of feature maps and x_k^l is feature point from E_l. p is the reference point where decoder extracts image features from. We modify the representation of p by adding an extra angle dimension to estimate original position and angle of original object query as $p_{(c,w,h,\alpha)}$ (c is the center point, w, h, α are width, height and angle of estimation of object queries). The object queries then will be fed into detection head for detection task.

Detection Head. After conducting cross-attention between the object query and the encoded image features, we can obtain the updated features $D \in \mathbb{R}^{N \times C}$ (N is the length of object queries). In the detection head, a 3-layer MLP and a linear layer are used to predict the bounding box and classification confidence. Different from original detection head in DETR (Carion et al., 2020), as for bounding boxes, we project the features D into 5-dimensional boxes including center point $x_c.y_c$, width and height w, h and the angle of bounding box α. We denote the prediction as

$$Box_{\{x_c,y_c,w,h,\alpha\}} = \textbf{Sigmoid}(\textbf{MLP}(D)), \\ Score = \textbf{FC}(D). \tag{6}$$

3.3 Fine-tune O^{2}DETR

The O^{2}DETR can be a new baseline model replacing Faster R-CNN (Ren et al., 2016) and RetinaNet (Lin et al., 2017b) for the oriented object detection problem. As is known, many methods are introduced into the two baseline models to refine detectors and refresh the SOTA performance. The O^{2}DETR opens up great possibilities of exploiting advantages of end-to-end oriented object detectors, thanks to its simple architecture-construction process, multi-scale visual expression and

fast convergence. Motivated by this, we provide an insight of improving performance of our new Transformer baseline by a simple yet effective fine-tuning strategy.

Inspired by the observation of high recall rate of O^2DETR revealed in Table 3, we establish a fine-tune network by exploiting O^2DETR as a region proposal generator. To save memory and computational cost, we freeze the parameters of O^2DETR, just fine-tune an additional prediction head for final bounding boxes and confidence scores. We regard the inferred bounding boxes of O^2DETR as region proposals, utilizing an Region of Interest Align (ROIAlign) network to project the proposals into feature maps obtained from backbone. The features aligned by ROIAlign would be fed into a prediction head for more accurate predictions of boxes and scores. The process can be formulated as

$$
\begin{aligned}
F &= \textbf{ROIAlign}(P, \{x^l\}_{l=1}^{L-1}), \\
Box^F_{\{x_c, y_c, w, h, \alpha\}} &= \textbf{Sigmoid}(\textbf{MLP}(F)), \\
Score^F &= \textbf{FC}(F), \\
\textbf{Box} &= Box_{\{x_c, y_c, w, h, \alpha\}} + Box^F_{\{x_c, y_c, w, h, \alpha\}},
\end{aligned}
\tag{7}
$$

where the F is the fine-tuned features and $Box^F_{\{x_c, y_c, w, h, \alpha\}}$, $Score^F$ are predictions of fine-tuned features. We calculate the bounding boxes of fine-tuned features as the residual of original location estimation and add it into the original bounding boxes generated by O^2DETR. No NMS is applied before feeding the region proposals to the ROIAlign. The fine-tune process is illustrated in Fig. 2.

4 Experiments

Dataset. We conduct experiments on DOTA (Xia et al., 2018), which is the benchmark dataset of oriented object detection. DOTA contains 2806 aerial images with the size ranges from 800×800 to 4000×4000 and 188282 instances with different scales, orientations and shapes of 15 common object categories, which includes: Plane (PL), Baseball diamond (BD), Bridge (BR), Ground track field (GTF), Small vehicle (SV), Large vehicle (LV), Ship (SH), Tennis court (TC), Basketball court (BC), Storage tank (ST), Soccer-ball field (SBF), Roundabout (RA), Harbor (HA), Swimming pool (SP), and Helicopter (HC). The fully annotated DOTA are divided into three parts: half of the images are randomly selected as training set, $1/6$ as the validation set and $1/3$ as the testing set. We crop original images into 1024×1024 patches with a stride of 824. We only adopt random horizontal flipping during training to avoid over-fitting and no other tricks are utilized if not specified.

Implentation Details. ImageNet (Deng et al., 2009) pre-trained ResNet-50 (He et al., 2016) is utilized as the backbone for ablations. In ablations, we denote models extracting features with ResNet-50 and ResNet-101 as O^2DETR-R50 and O^2DETR-R101, respectively. The fine-tuned model is denoted as F-O^2DETR. Multi-scale feature maps are extracted without FPN (Lin et al., 2017a). We use downsampling ratio of $64, 32, 16, 8$ to process feature maps by default. We set the length of object queries as 1000 as objects are always dense in DOTA image.

Performance trained for 50 epochs are reported and the learning rate drops to $1/10$ of its original value at the $40th$ epoch. When training the O^2DETR, the learning rate is set as 10^{-4} for the Transformer encoder-decoder and 10^{-5} for the pre-trained ResNet backbone. O^2DETR is trained by minimizing the classification loss, bounding box L1 loss, and IoU loss with coefficients $2, 5, 2$, respectively. In Transformer layers, post-normalization is adopted. We use random crop in training with the largest width or height set as 1024 for all ablations. During fine-tuning, we train the model for 1x (12 epochs) by default. All models are trained on NVIDIA Tesla $8\times$V100 GPUs with 2 images per GPU.

4.1 Comparison with Faster R-CNN and RetinaNet

Rotated Faster R-CNN (Ren et al., 2016) and RetinaNet (Lin et al., 2017b) are the most popular two-stage and one-stage baseline used in oriented object detection domain. Despite the differences in training scheme of anchor-based detectors and Transformer ones, we attempt to compare our O^2DETR baseline with them in a relative fair way. To align with O^2DETR, we train the rotated Faster R-CNN and RetinaNet for 3x schedule. Results are report in Table 1. Data augmentation is not used in all baselines. To be comparable, our O^2DETR uses 6 encoder layers and 6 decoder layers

with around 41M parameters using multi-scale features and ResNet-50. To the best of our knowledge, no rotated Transformer baseline has been presented in oriented object detection problem. O^2DETR has better performance in mAP compared with anchor-based baseline detectors when the number of parameters is similar. In conclusion, our proposed O^2DETR could serve as a strong and competitive baseline for oriented object detection problem.

Method	backbone	MS.dowsnsample ratios					Epochs	params	mAP
		64	32	16	8	4			
Faster R-CNN	ResNet-50						50	39M	60.32
(Ren et al., 2016)	ResNet-50	✓	✓	✓	✓		50	42M	64.17
	ResNet-50	✓	✓	✓	✓	✓	50	43M	66.25
	ResNet-101						50	60M	62.44
	ResNet-101	✓	✓	✓	✓		50	63M	66.03
	ResNet-101	✓	✓	✓	✓	✓	50	64M	67.71
RetinaNet	ResNet-50						50	34M	58.54
(Lin et al., 2017b)	ResNet-50	✓	✓	✓	✓		50	37M	62.78
	ResNet-50	✓	✓	✓	✓	✓	50	38M	65.77
	ResNet-101						50	55M	60.47
	ResNet-101	✓	✓	✓	✓		50	58M	64.11
	ResNet-101	✓	✓	✓	✓	✓	50	59M	66.53
O^2DETR	ResNet-50						50	38M	62.22
	ResNet-50	✓	✓	✓	✓		50	41M	66.10
	ResNet-50	✓	✓	✓	✓	✓	50	42M	68.65
	ResNet-101						50	59M	64.32
	ResNet-101	✓	✓	✓	✓		50	62M	67.66
	ResNet-101	✓	✓	✓	✓	✓	50	63M	70.02

Table 1: Comparisons with other baselines. (MS.downsample ratios mean downsampling ratio of multi-scale features)

4.2 Ablations

Depthwise Separable Convolution. We evaluate the influence of Depthwise Separable Convolution (DSConv for abbreviation) by comparing encoder of DSConv and encoder of self-attention mechanism (Table 2, O^2DETR-Attn represents using self-attention mechanism in encoder and O^2DETR-DSConv represents depthwise separable convolution). The implementation of O^2DETR-Attn and O^2DETR-DSConv keep the same except the components of encoder. The number of layers for both DSConv and attention encoder keeps the same as 6 and all models adopt multi-scale features with the downsampling ratio of $64, 32, 16, 8$. The results could prove the hypothesis that despite attention mechanisms use global scene reasoning in the whole image, in dense, tiny objects, local scene reasoning around objects is enough and even better, where local aggregation is the advantage of depthwise separable convolution.

Method	backbone	Epochs	param	mAP
O^2DETR-Attn	ResNet-50	50	43M	65.33
O^2DETR-Attn	ResNet-101	50	64M	66.45
O^2DETR-DSConv	ResNet-50	50	41M	66.10
O^2DETR-DSConv	ResNet-101	50	62M	67.66

Table 2: Comparisons between self-attention mechanism (**Transformer**) and depthwise separable convolution in encoder of O^2DETR.

Fine-tune on O^2DETR. To be comparable with other detectors based on baseline of Faster R-CNN (Ren et al., 2016) and RetinaNet (Lin et al., 2017b), we propose to fine-tune the O^2DETR by utilizing O^2DETR as a region proposal network. The theoretical foundation of effectiveness

of such fine-tune method is the high recall rate we report on Table 3. We compute the recall of proposals at different IoU ratios with ground-truth boxes. The Recall-to-IoU metric is not strictly related to the ultimate detection accuracy, but it is an important metric to evaluate the proposal performance. Compared with the RPN of Faster R-CNN (Ren et al., 2016), our model has higher recall rate, indicating our model covers more positive proposals. Different from original RPN, we keep the parameters of O^2DETR fixed to act as an inference network. The proposals predicted by the inference network would be used into feature maps and finely modify bounding boxes and classifications to acquire better performance.

		IoU		
Method	0.2	0.3	0.4	0.5
RPN	47.86	44.22	39.98	35.11
O^2DETR	68.49	68.09	67.17	65.27

Table 3: Recall rates of RPN in Faster R-CNN (Ren et al., 2016) and O^2DETR.

Method	backbone	Epochs	Fine-tune Epochs	mAP
O^2DETR	ResNet-50	50	0	66.10
O^2DETR	ResNet-101	50	0	67.66
F-O^2DETR	ResNet-50	50	12	74.47
F-O^2DETR	ResNet-101	50	12	76.23

Table 4: Effectiveness of fine-tune.

As is shown in Table 4, the fine-tuning method improves the mAP performance largely by adding negligible extra fine-tuning epochs. All the models shown in Table 4 adopt multi-scale features with downsampling ratio $64, 32, 16, 8$. The boost of performance demonstrates using O^2DETR as the baseline is feasible and has great potential. Other attempts are welcomed to be introduced to raise detection accuracy based on our baseline.

4.3 Comparison with the State-of-the-art

In this section, we compare our proposed O^2DETR with other state-of-the-art methods on an aerial oriented object detection dataset DOTA. The settings of our model have been introduced in Implementation Details. We achieve 74.47% and 79.66% mAP with ResNet-50-FPN backbone by fine-tuning the O^2DETR using single-scale and multi-scale dataset, respectively. In Table 5, we report specific mAP performance in each categories (PL-plane, BD-baseball diamond, BR-bridge, GTF-ground track field, SV-small vehicle, LV-large vehicle, SH-ship, TC-tennis court, BC-basketball court, ST-storage tank, SBF-soccer ball field, RA-roundabout, HA-harbor, SP-swimming pool, HC-helicopter).

By simply fine-tuning the O^2DETR, the performance is quite competitive compared with SOTA performance. It illustrates our fine-tuned model performs better than S^2ANet (Han et al., 2020) as backbone is ResNet-50 with FPN. The SOTA performance, ReDet (Han et al., 2021), retraining models backbone based on ResNet-50 and is not strictly comparable with other our model and S^2ANet.

We show some qualitative samples in Fig. 3. The visualization of detpth-wise encoding in the third row of Fig. 3. We visualize the activation map of encoded features after depthwise convolution. The activation map will emphasize dense object region in input image. Compared with the global reasoning of attention mechanism, the local aggregation is enough to refer the targets in a less complex way.

5 Conclusion

In this paper, we propose a new end-to-end model, O^2DETR, for oriented object detection problem via Transformer. The O^2DETR outperforms original rotated Faster R-CNN and RetinaNet baseline

Method	backbone	PL	BD	BR	GTF	SV	LV	SH	TC	BC	ST	SBF	RA	HA	SP	HC	mAP
single-scale																	
FR-O	R101	79.42	77.13	17.70	64.05	35.50	38.02	37.16	89.41	69.64	59.28	50.30	52.91	47.89	47.40	46.30	54.13
ICN	R101-FPN	81.36	74.30	47.70	70.32	64.89	67.82	69.98	90.76	79.06	78.20	53.64	62.90	67.02	64.17	50.23	68.16
CADNet	R101-FPN	87.80	82.40	49.40	73.50	71.10	63.50	76.60	90.90	79.20	73.30	48.40	60.90	62.00	67.00	62.20	69.90
DRN	H-104	88.91	80.22	43.52	63.35	73.48	70.69	84.94	90.14	83.85	84.11	50.12	58.41	67.62	68.60	52.50	70.70
CenterMap	R50-FPN	88.88	81.24	53.15	60.65	78.62	66.55	78.10	88.83	77.80	83.61	49.36	66.19	72.10	72.36	58.70	71.74
SCRDet	R101-FPN	89.98	80.65	52.09	68.36	68.36	60.32	72.41	90.85	87.94	86.86	65.02	66.68	66.25	68.24	65.21	72.61
R^3Det	R152-FPN	89.49	81.17	50.53	66.10	70.92	78.66	78.21	90.81	85.26	84.23	61.81	63.77	68.16	69.83	67.17	73.74
S^2ANet	R50-FPN	89.11	82.84	48.37	71.11	78.11	78.39	87.25	90.83	84.90	85.64	60.36	62.60	65.26	69.13	57.94	74.12
ReDet	ReR50-ReFPN	88.79	82.64	53.97	74.00	78.13	84.06	88.04	90.89	87.78	85.75	61.76	60.39	75.96	68.07	63.59	76.25
O^2DETR	R50-FPN	83.89	75.11	44.04	64.20	78.39	76.78	87.68	90.60	78.58	71.82	53.21	60.35	55.36	61.90	47.89	68.65
F-O^2DETR	R50-FPN	88.76	81.91	51.20	72.18	77.64	80.47	87.84	90.85	84.56	81.68	61.42	64.61	67.50	64.28	62.15	74.47
multi-scale																	
ROI Trans	R101-FPN	88.64	78.52	43.44	75.92	68.81	73.68	83.59	90.74	77.27	81.46	58.39	53.54	62.83	58.93	47.67	69.56
O^2-DNet	H104	89.30	83.30	50.10	72.10	71.10	75.60	78.70	90.90	79.90	82.90	60.20	60.00	64.60	68.90	65.70	72.80
DRN	H104	89.71	82.34	47.22	64.10	76.22	74.43	85.84	90.57	86.18	84.89	57.65	61.93	69.30	69.63	58.48	73.23
Gliding Vertex	R101-FPN	89.64	85.00	52.26	77.34	73.01	73.14	86.82	90.74	79.02	86.81	59.55	70.91	72.94	70.86	57.32	75.02
BBAVectors	R101	88.63	84.06	52.13	69.56	78.26	80.40	88.06	90.87	87.23	86.39	56.11	65.62	67.10	72.08	63.96	75.36
CenterMap	R101-FPN	89.83	84.41	54.60	70.25	77.66	78.32	87.19	90.66	84.89	85.27	56.46	69.23	74.13	71.56	66.06	76.03
CSL	R152-FPN	90.25	85.53	54.64	75.31	70.44	73.51	77.62	90.84	86.15	86.69	69.60	68.04	73.83	71.10	68.93	76.17
SCRDet++	R152-FPN	88.68	85.22	54.70	73.71	71.92	84.14	79.39	90.82	87.04	86.02	67.90	60.86	74.52	70.76	72.66	76.56
S^2ANet	R50-FPN	88.89	83.60	57.74	81.95	79.94	83.19	89.11	90.78	84.87	87.81	70.30	68.25	78.30	77.01	69.58	79.42
ReDet	ReR50-ReFPN	88.81	82.48	60.83	80.82	78.34	86.06	88.31	90.87	88.77	87.03	68.65	66.90	79.26	79.71	74.67	80.10
O^2DETR	R50-FPN	86.01	75.92	46.02	66.65	79.70	79.93	89.17	90.44	81.19	76.00	56.91	62.45	64.22	65.80	58.96	72.15
F-O^2DETR	R50-FPN	88.89	83.41	56.72	79.75	79.89	85.45	89.77	90.84	86.15	87.66	69.94	68.97	78.83	78.19	70.38	79.66

Table 5: Comparison with state-of-the-art methods on DOTA. R-50(101)-FPN stands for ResNet-50(101) with FPN and H104 stands for Hourglass-104. F-O^2DETR means fine-tuned O^2DETR. Multi-scale indicates training and testing on multi-scale cropped images.
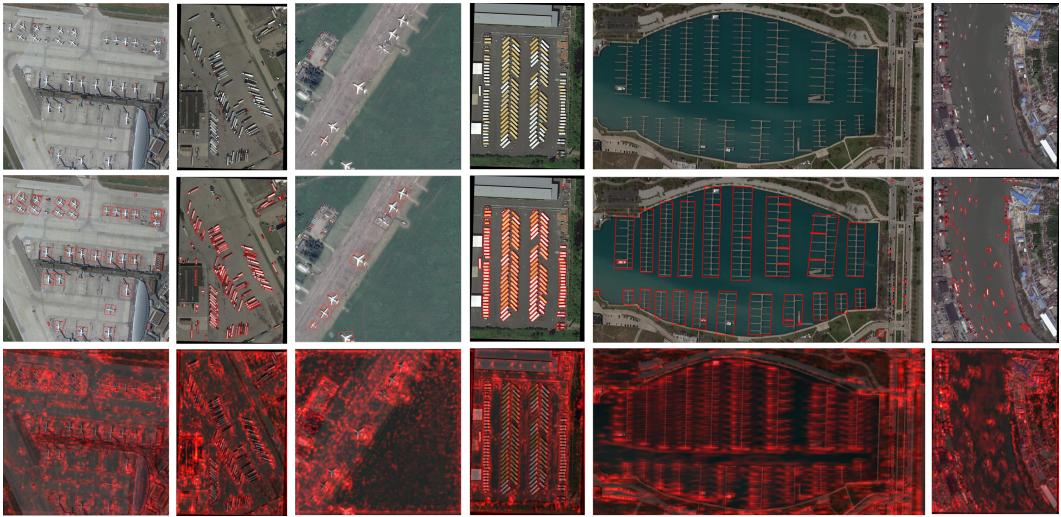

Figure 3: Visualization of detecting with O^2DETR. The first row is images to be detected, and the second row is detection results of O^2DETR. The third row is visualization of depth-wise encoding.

on the challenging DOTA dataset. The O^2DETR is straightforward and flexible to apply in oriented object detection. Based on that, we provide a new method by fine-tuning O^2DETR to achieve a competitive performance compared with the state-of-the-arts. Extensive ablations on DOTA dataset demonstrate the effectiveness of our method. In the future work, we will try more applications to verify the performance of our method.

References

Iz Beltagy, Matthew E Peters, and Arman Cohan. Longformer: The long-document transformer. *arXiv preprint arXiv:2004.05150*, 2020.

Tom B Brown, Benjamin Mann, Nick Ryder, Melanie Subbiah, Jared Kaplan, Prafulla Dhariwal, Arvind Neelakantan, Pranav Shyam, Girish Sastry, Amanda Askell, et al. Language models are few-shot learners. *arXiv preprint arXiv:2005.14165*, 2020.

Nicolas Carion, Francisco Massa, Gabriel Synnaeve, Nicolas Usunier, Alexander Kirillov, and Sergey Zagoruyko. End-to-end object detection with transformers. In *European Conference on Computer Vision*, pages 213–229, 2020.

François Chollet. Xception: Deep learning with depthwise separable convolutions. In *Proceedings of the IEEE/CVF Conference on Computer Vision and Pattern Recognition*, pages 1251–1258, 2017.

Jia Deng, Wei Dong, Richard Socher, Li-Jia Li, Kai Li, and Li Fei-Fei. Imagenet: A large-scale hierarchical image database. In *Proceedings of the IEEE/CVF Conference on Computer Vision and Pattern Recognition*, 2009.

Jacob Devlin, Ming-Wei Chang, Kenton Lee, and Kristina Toutanova. Bert: Pre-training of deep bidirectional transformers for language understanding. *arXiv preprint arXiv:1810.04805*, 2018.

Jian Ding, Nan Xue, Yang Long, Gui-Song Xia, and Qikai Lu. Learning roi transformer for oriented object detection in aerial images. In *Proceedings of the IEEE/CVF Conference on Computer Vision and Pattern Recognition*, pages 2849–2858, 2019.

Alexey Dosovitskiy, Lucas Beyer, Alexander Kolesnikov, Dirk Weissenborn, Xiaohua Zhai, Thomas Unterthiner, Mostafa Dehghani, Matthias Minderer, Georg Heigold, Sylvain Gelly, et al. An image is worth 16×16 words: Transformers for image recognition at scale. 2020.

Peng Gao, Zhengkai Jiang, Haoxuan You, Pan Lu, Steven CH Hoi, Xiaogang Wang, and Hongsheng Li. Dynamic fusion with intra-and inter-modality attention flow for visual question answering. In *Proceedings of the IEEE/CVF Conference on Computer Vision and Pattern Recognition*, pages 6639–6648, 2019a.

Peng Gao, Haoxuan You, Zhanpeng Zhang, Xiaogang Wang, and Hongsheng Li. Multi-modality latent interaction network for visual question answering. In *Proceedings of the IEEE/CVF International Conference on Computer Vision*, pages 5825–5835, 2019b.

Peng Gao, Chiori Hori, Shijie Geng, Takaaki Hori, and Jonathan Le Roux. Multi-pass transformer for machine translation. *arXiv preprint arXiv:2009.11382*, 2020.

Peng Gao, Minghang Zheng, Xiaogang Wang, Jifeng Dai, and Hongsheng Li. Fast convergence of detr with spatially modulated co-attention. *arXiv preprint arXiv:2101.07448*, 2021.

Shijie Geng, Peng Gao, Moitreya Chatterjee, Chiori Hori, Jonathan Le Roux, Yongfeng Zhang, Hongsheng Li, and Anoop Cherian. Dynamic graph representation learning for video dialog via multi-modal shuffled transformers. *arXiv preprint arXiv:2007.03848*, 2020.

Jiaming Han, Jian Ding, Jie Li, and Gui-Song Xia. Align deep features for oriented object detection. *arXiv preprint arXiv:2008.09397*, 2020.

Jiaming Han, Jian Ding, Nan Xue, and Gui-Song Xia. Redet: A rotation-equivariant detector for aerial object detection. *arXiv preprint arXiv:2103.07733*, 2021.

Kaiming He, Xiangyu Zhang, Shaoqing Ren, and Jian Sun. Deep residual learning for image recognition. In *Proceedings of the IEEE/CVF Conference on Computer Vision and Pattern Recognition*, pages 770–778, 2016.

Andrew G Howard, Menglong Zhu, Bo Chen, Dmitry Kalenichenko, Weijun Wang, Tobias Weyand, Marco Andreetto, and Hartwig Adam. Mobilenets: Efficient convolutional neural networks for mobile vision applications. *arXiv preprint arXiv:1704.04861*, 2017.

Yingying Jiang, Xiangyu Zhu, Xiaobing Wang, Shuli Yang, Wei Li, Hua Wang, Pei Fu, and Zhenbo Luo. R2cnn: rotational region cnn for orientation robust scene text detection. *arXiv preprint arXiv:1706.09579*, 2017.

Angelos Katharopoulos, Apoorv Vyas, Nikolaos Pappas, and François Fleuret. Transformers are rnns: Fast autoregressive transformers with linear attention. In *International Conference on Machine Learning*, pages 5156–5165. PMLR, 2020.

Nikita Kitaev, Łukasz Kaiser, and Anselm Levskaya. Reformer: The efficient transformer. *arXiv preprint arXiv:2001.04451*, 2020.

Tsung-Yi Lin, Piotr Dollár, Ross Girshick, Kaiming He, Bharath Hariharan, and Serge Belongie. Feature pyramid networks for object detection. In *Proceedings of the IEEE/CVF Conference on Computer Vision and Pattern Recognition*, pages 2117–2125, 2017a.

Tsung-Yi Lin, Priya Goyal, Ross Girshick, Kaiming He, and Piotr Dollár. Focal loss for dense object detection. In *Proceedings of the IEEE international conference on computer vision*, pages 2980–2988, 2017b.

Jiasen Lu, Dhruv Batra, Devi Parikh, and Stefan Lee. Vilbert: Pretraining task-agnostic visiolinguistic representations for vision-and-language tasks. 2019.

Jianqi Ma, Weiyuan Shao, Hao Ye, Li Wang, Hong Wang, Yingbin Zheng, and Xiangyang Xue. Arbitrary-oriented scene text detection via rotation proposals. *IEEE Transactions on Multimedia*, 20(11):3111–3122, 2018.

Mingyuan Mao, Renrui Zhang, Honghui Zheng, Peng Gao, Teli Ma, Yan Peng, Errui Ding, and Shumin Han. Dual-stream network for visual recognition. *arXiv preprint arXiv:2105.14734*, 2021.

Myle Ott, Sergey Edunov, David Grangier, and Michael Auli. Scaling neural machine translation. *arXiv preprint arXiv:1806.00187*, 2018.

Alec Radford, Karthik Narasimhan, Tim Salimans, and Ilya Sutskever. Improving language understanding by generative pre-training. 2018.

Alec Radford, Jeffrey Wu, Rewon Child, David Luan, Dario Amodei, and Ilya Sutskever. Language models are unsupervised multitask learners. *OpenAI blog*, 1(8):9, 2019.

Prajit Ramachandran, Niki Parmar, Ashish Vaswani, Irwan Bello, Anselm Levskaya, and Jonathon Shlens. Stand-alone self-attention in vision models. *arXiv preprint arXiv:1906.05909*, 2019.

Shaoqing Ren, Kaiming He, Ross Girshick, and Jian Sun. Faster r-cnn: towards real-time object detection with region proposal networks. *IEEE transactions on pattern analysis and machine intelligence*, 39(6):1137–1149, 2016.

Laurent Sifre and Stéphane Mallat. Rotation, scaling and deformation invariant scattering for texture discrimination. In *Proceedings of the IEEE/CVF Conference on Computer Vision and Pattern Recognition*, pages 1233–1240, 2013.

Ashish Vaswani, Noam Shazeer, Niki Parmar, Jakob Uszkoreit, Llion Jones, Aidan N Gomez, Lukasz Kaiser, and Illia Polosukhin. Attention is all you need. In *NIPS*, 2017.

Sinong Wang, Belinda Li, Madian Khabsa, Han Fang, and Hao Ma. Linformer: Self-attention with linear complexity. *arXiv preprint arXiv:2006.04768*, 2020.

Gui-Song Xia, Xiang Bai, Jian Ding, Zhen Zhu, Serge Belongie, Jiebo Luo, Mihai Datcu, Marcello Pelillo, and Liangpei Zhang. Dota: A large-scale dataset for object detection in aerial images. In *Proceedings of the IEEE/CVF Conference on Computer Vision and Pattern Recognition*, pages 3974–3983, 2018.

Xue Yang and Junchi Yan. Arbitrary-oriented object detection with circular smooth label. In *European Conference on Computer Vision*, pages 677–694, 2020.

Xue Yang, Qingqing Liu, Junchi Yan, Ang Li, Zhiqiang Zhang, and Gang Yu. R3det: Refined single-stage detector with feature refinement for rotating object. *arXiv preprint arXiv:1908.05612*, 2019a.

Xue Yang, Jirui Yang, Junchi Yan, Yue Zhang, Tengfei Zhang, Zhi Guo, Xian Sun, and Kun Fu. Scrdet: Towards more robust detection for small, cluttered and rotated objects. In *Proceedings of the IEEE International Conference on Computer Vision*, pages 8232–8241, 2019b.

Zhou Yu, Jun Yu, Yuhao Cui, Dacheng Tao, and Qi Tian. Deep modular co-attention networks for visual question answering. In *Proceedings of the IEEE/CVF Conference on Computer Vision and Pattern Recognition*, pages 6281–6290, 2019.

Minghang Zheng, Peng Gao, Xiaogang Wang, Hongsheng Li, and Hao Dong. End-to-end object detection with adaptive clustering transformer. *arXiv preprint arXiv:2011.09315*, 2020.

Lin Zhou, Haoran Wei, Hao Li, Wenzhe Zhao, Yi Zhang, and Yue Zhang. Objects detection for remote sensing images based on polar coordinates. *arXiv preprint arXiv:2001.02988*, 2020.

Xizhou Zhu, Weijie Su, Lewei Lu, Bin Li, Xiaogang Wang, and Jifeng Dai. Deformable detr: Deformable transformers for end-to-end object detection. *arXiv preprint arXiv:2010.04159*, 2020.